

# Application of Microelectrode Voltammetry to Study the Properties of Surfactant Solutions: Alkyltrimethylammonium Bromides

Tiago L. Ferreira,<sup>†</sup> Bruno M. Sato,<sup>‡</sup> Omar A. El Seoud,<sup>‡</sup> and Mauro Bertotti<sup>\*,‡</sup>

Departamento de Ciências Exatas e da Terra, Universidade Federal de São Paulo, São Paulo, SP, Brazil, and Instituto de Química, Universidade de São Paulo, São Paulo, SP, Brazil

Received: October 8, 2009; Revised Manuscript Received: November 6, 2009

Microelectrode cyclic voltammetry (MV) has been employed to investigate the micellar properties of solutions of homologous alkyltrimethylammonium bromides,  $\text{RMe}_3\text{ABr}$ ,  $\text{R} = \text{C}_{10}$ ,  $\text{C}_{12}$ , and  $\text{C}_{14}$ , in water and in the presence of added NaBr. The micellar self-diffusion coefficient was calculated from the limiting current for the reversible electron transfer of micelle-bound ferrocene. From the values of this property, other parameters were calculated, including the micellar hydrodynamic radius,  $R_{\text{H}}$ , and aggregation number,  $N_{\text{agg}}$ ; the latter was also theoretically calculated. We determined the values of the diffusion coefficient as a function of various experimental variables and observed the following trends: The diffusion coefficient decreases as a function of increasing surfactant concentration (no additional electrolyte added); it decreases as a function of increasing surfactant concentration at fixed NaBr concentration; and it shows a complex dependence (increase then decrease) on the NaBr concentration at a fixed  $\text{RMe}_3\text{ABr}$  concentration. The value of the intermicellar interaction parameter decreases and then increases as a function of increasing NaBr concentration. These results are discussed in terms of intermicellar interactions and the effect of NaBr on the micellar surface charge density and sphere-to-rod geometry change. The NaBr concentration required to induce the latter change increases rapidly as a function of decreasing the length of R: no geometry change was detected for  $\text{C}_{10}\text{Me}_3\text{ABr}$ . Values of  $N_{\text{agg}}$  increase as a function of increasing the length of R and are in good agreement with both literature values and values that were calculated theoretically. Thus, MV is a convenient and simple technique for obtaining fundamental properties of surfactant solutions, including additive-induced changes of micellar parameters ( $N_{\text{agg}}$ ) and morphology changes.

## Introduction

An illustrative example of the relevance of the properties of micellar solutions to their applications is viscosity. For ionic surfactants, this property can be readily changed, sometimes dramatically, by increasing the surfactant concentration or by adding electrolytes,<sup>1,2</sup> fatty alcohols,<sup>3</sup> fatty amines,<sup>4</sup> hydrocarbons,<sup>5</sup> or mixtures thereof. Considerable efforts have been made to elucidate the micellar structure under a variety of experimental conditions and to understand the phenomenological basis for micellar behavior at the microscopic level.<sup>6–8</sup> Calculation of the micellar diffusion coefficient,  $D_{\text{mic}}$ , sheds light on the changes in micellar structure as a function of experimental variables such as the concentrations of both the surfactant and added electrolytes or the temperature.<sup>9,10</sup> Scattering techniques (light and neutron) have been employed to calculate mutual diffusion coefficients,<sup>11–13</sup> whereas Taylor dispersion<sup>14</sup> and spin-echo NMR spectroscopy<sup>15</sup> yield self-diffusion data. The main difference between these coefficients is that the latter is obtained under conditions where a concentration gradient of the species is not created, that is, interactions among the particles are taken into account.<sup>14,15</sup>

Micellar self-diffusion coefficients,  $D_{\text{mic}}$ , have been obtained by electrochemical techniques through the use of micelle-solubilized electroactive probes, such as ferrocene (Supporting Information).<sup>16–24</sup> Additionally, these techniques yield information on the hydrodynamic radius,  $R_{\text{H}}$ ; the aggregation number,

$N_{\text{agg}}$ ; and interparticle interactions in micellar solution. Microelectrode voltammetry, MV, is attractive because the measurements are obtained under steady-state conditions in quiescent solutions.<sup>20–24</sup> Although hydrodynamic techniques, such as rotating-electrode voltammetry, yield similar information, the micellar geometry can be significantly influenced by forced convection, and if this occurs, it adversely affects the experimental results.

Electroactive probes should have a high affinity for the hydrophobic core of the micelle. Additionally, their size should be compatible with that of the micelle, in order not to disturb the aggregate. Ferrocene is the most often employed electroactive probe, because of its favorable characteristics, including well-known electrochemical behavior<sup>25,26</sup> and high hydrophobic character.<sup>27</sup> Other molecules have also been utilized as electrochemical probes.<sup>28–30</sup>

Micellar structure and intermicellar interactions are affected by experimental variables, including surfactant molecular structure, charge, and concentration; presence and concentration of additives, if any; temperature; and shear conditions of the solution.<sup>31–33</sup> Even at concentrations above, but not far from, the critical micelle concentration (cmc) micelles mutually interact; consequently, the calculated values of diffusion coefficients are lower than that at the cmc. As attenuation of the mass-transport parameters is a linear function of surfactant concentration, linear interaction theory applies.<sup>34</sup> Consequently, extrapolation to infinite dilution (to the cmc) yields mass-transport parameters that are independent of interparticle interactions

\* Corresponding author. Fax: 5511-3815-557. E-mail: mbertott@iq.usp.br.

<sup>†</sup> Universidade Federal de São Paulo.

<sup>‡</sup> Universidade de São Paulo.

$$D_{\text{obs}} = D_{\text{cmc}}[1 - k_D(C_{\text{surf}} - \text{cmc})] \quad (1)$$

where  $D_{\text{obs}}$  is the observed micellar diffusion coefficient,  $D_{\text{cmc}}$  is the micellar diffusion coefficient at the cmc,  $C_{\text{surf}}$  is the total surfactant concentration, and  $k_D$  is the intermicellar interaction coefficient. Note that  $D_{\text{obs}}$  denotes the micellar diffusion coefficient ( $D_{\text{mic}}$ ) under any experimental conditions, except at  $C_{\text{surf}} = \text{cmc}$ , in the absence of added NaBr. It is important to note that the cmc decreases with increasing bromide concentration, so cmc values should be determined at each bromide concentration examined. Nevertheless, as cmc values are much smaller than the surfactant concentrations employed in the experiments, the variation of the cmc value does not affect the difference term in eq 1. Therefore, the cmc values are determined only in the absence of bromide for all surfactants.

The value of  $R_H$  is then calculated from the Stokes–Einstein equation

$$D = \frac{kT}{6\pi\eta R_H} \quad (2)$$

where  $kT$  has its usual meaning;  $\eta$  is the solution viscosity at the cmc; and  $D$  stands for  $D_{\text{cmc}}$  or  $D_{\text{mic}}$ , depending on the experimental conditions. Equation 2 is derived by considering a liquid flow past a hard sphere,<sup>35</sup> with the stick boundary conditions that the flow is zero on the surface of the sphere. Knowing the value of  $R_H$  allows calculation of  $N_{\text{agg}}$ .

Recently, we applied MV to study the micellar properties of  $\text{C}_{16}\text{Me}_3\text{ABr}$ , as well as the effects of KBr on the aggregates formed.<sup>23</sup> We have now extended this study to other members of this class of surfactants, namely,  $\text{C}_{10}\text{Me}_3\text{ABr}$ ,  $\text{C}_{12}\text{Me}_3\text{ABr}$ , and  $\text{C}_{14}\text{Me}_3\text{ABr}$ . In addition to the determination of the above-mentioned micellar parameters, this work shows, for the first time, the application of MV to study the effects of increasing the length of the surfactant hydrophobic tail on micellar parameters, interparticle interactions, and sphere-to-rod geometry changes.

## Experimental Section

**Materials.** The surfactants were synthesized by reaction of the appropriate *N,N*-dimethylalkylamine with methyl iodide, followed by  $\text{I}^-/\text{Br}^-$  ion exchange. The tertiary amines were obtained by the reductive amination of purified alkylamines with a mixture of formaldehyde and formic acid.<sup>36</sup> A mixture of 0.1 mol of the tertiary amine and 0.115 mol of  $\text{CH}_3\text{I}$  was refluxed in 100 mL of acetone for 2 h, after which the solvent was evaporated and the product was washed with cold acetone. The product was dissolved in ethanol and passed through a column containing 130 mL of Purolite SGA-550-OH anion-exchange

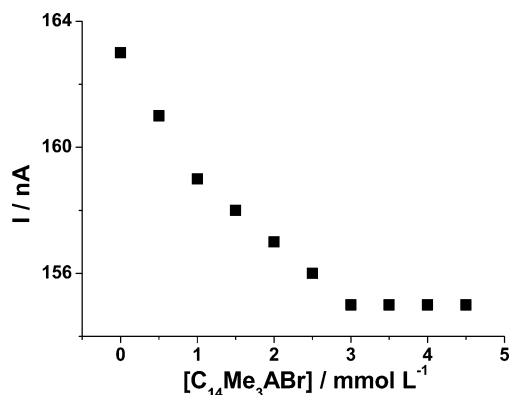


**Figure 1.** Representative plot for the determination of the cmc by microelectrode cyclic voltammetry.

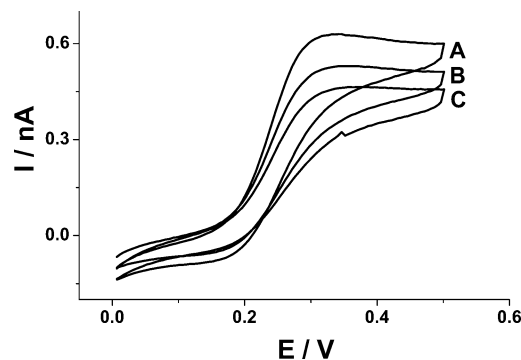


**Figure 2.** Cyclic voltammograms for ferrocene/ $\text{C}_{14}\text{Me}_3\text{ABr}$  solutions, recorded with a platinum disk microelectrode. Concentrations are given in  $\text{mol L}^{-1}$  for  $\text{C}_{14}\text{Me}_3\text{ABr}$ /ferrocene: (A) 0.111/0.00145, (B) 0.093/0.00120, (C) 0.074/0.00095. Scan rate =  $50 \text{ mV s}^{-1}$ .

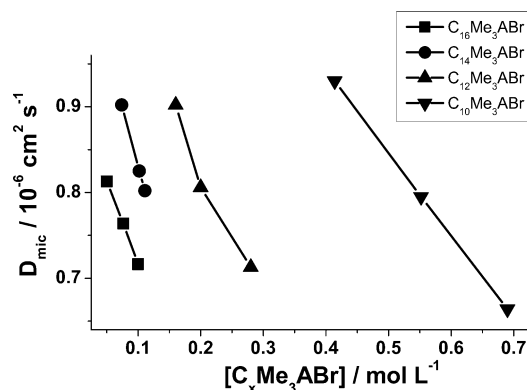


**Figure 3.** Relationship between  $D$  and surfactant concentration for  $\text{C}_{10}$ - to  $\text{C}_{16}\text{Me}_3\text{ABr}$  in the absence of bromide.

**TABLE 1: cmc Values of Alkyltrimethylammonium Bromides**

surfactant	cmc ( $\text{mmol L}^{-1}$ )	
	from voltammetry	from the literature
$\text{C}_{10}\text{Me}_3\text{ABr}$	$42 \pm 6$	$69,^{48} 60,^{44} 50,^{43} 57^{42}$
$\text{C}_{12}\text{Me}_3\text{ABr}$	$12 \pm 1$	$15,^{48} 13.3,^{44} 15,^{43} 14.5^{42}$
$\text{C}_{14}\text{Me}_3\text{ABr}$	$2.7 \pm 0.3$	$3.5,^{48} 3.0,^{44} 4,^{43} 3.8^{42}$
$\text{C}_{16}\text{Me}_3\text{ABr}$	$0.70 \pm 0.05$	$0.87,^{48} 1,^{43} 0.89^{42}$

resin (ca. 150 mequiv). The eluted surfactant solution was tested for the absence of iodide ion.<sup>37</sup> All bromide surfactants were recrystallized from an acetone/methanol mixture and were dried prior to use. Plots (not shown) of surface tension versus the logarithm of the surfactant concentration showed that the compounds prepared were surface-active pure (Lauda TE1C digital ring tensiometer,  $25^\circ\text{C}$ ).

Ferrocene (Eastman-Kodak) and NaBr (Aldrich, analytical grade) were employed as received. Probe stock solutions were prepared by dissolving the appropriate amount of the solid in the surfactant solution. Distilled, deionized water was used throughout (Nanopure Infinity water purification system, Barnstead, Dubuque, IA).

**Voltammetric Measurements.** Voltammetric measurements were carried out with an Autolab PGSTAT 30 potentiostat (Eco Chemie, Utrecht, The Netherlands) using the three-electrode mode. Platinum disk microelectrodes were constructed by attaching platinum microfibers (diameter =  $25 \mu\text{m}$ ) to glass capillaries. To ensure reproducible measurements, microelectrodes were polished with an alumina slurry and thoroughly washed with water prior to use. A platinum wire was used as the auxiliary electrode, and the reference electrode was a home-

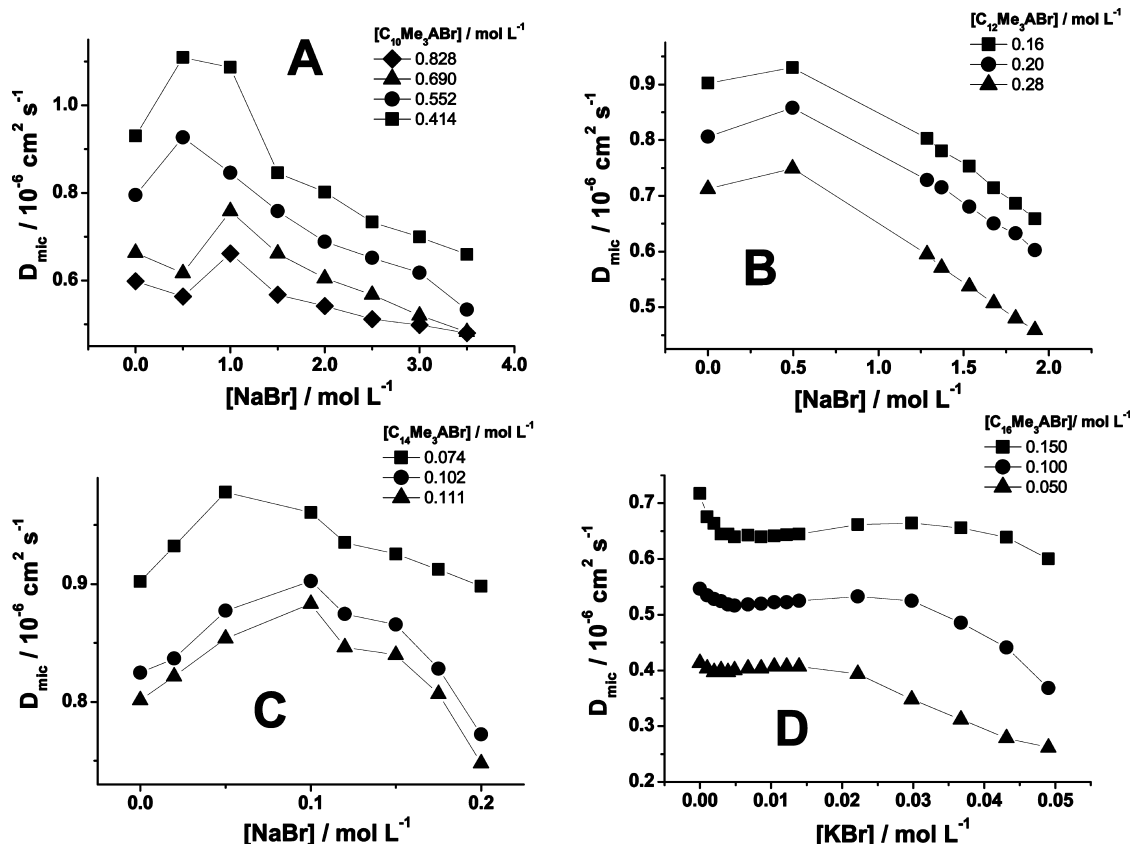


**Figure 4.** Dependence of (A)  $C_{10}Me_3ABr$ , (B)  $C_{12}Me_3ABr$ , (C)  $C_{14}Me_3ABr$ , and (D)  $C_{16}Me_3ABr$  micellar diffusion coefficients on bromide concentration.

constructed Ag/AgCl (KCl-saturated) electrode.<sup>38</sup> Cyclic voltammetry was carried out with a potential sweep rate of 50 mV  $s^{-1}$ . All experiments were performed at a constant temperature of  $25.0 \pm 0.1$  °C.

Values of the appropriate diffusion constant  $D$  can be calculated from eq 3, applicable to disk microelectrodes under steady-state conditions<sup>39–41</sup>

$$I_L = 4nFC_{\text{elect}}D_{\text{elect}}r \quad (3)$$

where  $I_L$  is the limiting current;  $D_{\text{elect}}$  is the diffusion coefficient of the appropriate electroactive species (free or micelle-bound), whose concentration is  $C_{\text{elect}}$ ;  $r$  is the radius of the microdisk electrode; and  $n$  and  $F$  have their usual meanings. Equation 3 was employed for several purposes, the first of which was to calculate the value of  $r$  from the limiting currents, measured for standard solutions of ferricyanide in 0.1 mol  $L^{-1}$  KCl.<sup>39</sup> Once the microelectrode radius is known, values of the appropriate  $D$  coefficient for micelle-bound ferrocene can be readily calculated. Finally, we employed the same equation to calculate the solubility of ferrocene in water at 25 °C. Solid ferrocene was added to water, and the suspension was agitated for 24 h (tube rotator, model 099A, Glas-Col, Terre Haute, IN) and then filtered. A duplicate experiment indicated that the solubility is ca.  $9.8 \times 10^{-6}$  mol  $L^{-1}$ . This value is very similar to that reported by Mandal,<sup>27</sup>  $1.0 \times 10^{-5}$  mol  $L^{-1}$ .

The cmc values of all surfactants were also obtained by using MV.<sup>16</sup> Aqueous and micellar solutions of hexamine ruthenium(III) chloride were prepared, all containing a fixed concentration of the ruthenium compound, 18.0 mmol  $L^{-1}$ . The influence of the surfactant concentration on the limiting current of the electroactive species was determined; the cmc was taken

as the surfactant concentration at which a break was observed in the plot of  $I_L$  versus surfactant concentration.

**Theoretical Calculation of the Aggregation Numbers.** Calculations were performed using Gaussian 03, revision D.01 (Gaussian, Inc., Wallingford, CT) in two steps: For each surfactant cation, the geometry was first optimized in the gas phase, without imposing geometrical constraints, using the B3LYP hybrid density functional and the 6-311+G(d,p) basis set. Each species (gas-phase) was then used as input for geometry optimization in water, performed using the polarizable continuum model (PCM), the B3LYP density functional, and the 6-311+G(d,p) basis set. The length of the micellized monomer, henceforth called the micellar radius, was taken as the distance between the quaternary nitrogen and the farthest H of the terminal methyl group  $(CH_3)_3N^+-(CH_2)_nCH_3$ . The value of  $N_{\text{agg}}$  was calculated from this radius and the volume of the hydrated monomer, as calculated by the PCM, by assuming a spherical-shaped micellar aggregate. To decrease the uncertainty in volume calculations, all geometry optimizations were carried out by using the “tight option” calculation mode.

## Results and Discussion

Values of the cmc of  $C_xMe_3ABr$  were determined from plots of  $I_L$  for  $Ru(NH_3)_6^{3+}$  as a function of surfactant concentration. A representative plot is shown in Figure 1, and the results are listed in Table 1. Values of the cmc determined by voltammetry are slightly lower than those obtained by other techniques, such as calorimetry,<sup>42</sup> surface tension,<sup>43</sup> and conductivity.<sup>44</sup> Several factors can be invoked to explain this difference, including reduction of the chemical potential of the monomers because

**TABLE 2: Threshold Concentration of Salt Needed to Cause Sphere-to-Rod Transition**

surfactant	concentration of salt (mol L <sup>-1</sup> )
C <sub>16</sub> Me <sub>3</sub> ABr	0.01 (KBr) <sup>23,54</sup>
C <sub>16</sub> Me <sub>3</sub> ABr	0.02–0.05 (KCl) <sup>24</sup>
C <sub>16</sub> Me <sub>3</sub> ACl	1.2 (NaCl) <sup>19</sup>
C <sub>14</sub> Me <sub>3</sub> ABr	0.12 (NaBr) <sup>54</sup>
C <sub>12</sub> Me <sub>3</sub> ABr	1.8 (NaBr) <sup>55,56</sup>
C <sub>10</sub> Me <sub>3</sub> ABr	—

of their interaction with the ruthenium compound and ionic strength effects (screening) on the electrostatic repulsion between the monomer headgroups in the aggregate.<sup>45</sup> An additional factor is that the values of cmc are technique-dependent, as discussed elsewhere.<sup>46</sup> For example, Mukerjee and Mysels compiled 54 cmc values for C<sub>16</sub>NMe<sub>3</sub>ABr (measurements at 25 °C), differing, for the same technique, by as much as 22%.<sup>47</sup>

The main objective of the present work was to show that MV is a simple and convenient technique for studying one of the most important characteristics of homologous series of surfactants, namely, the dependence of the micellar properties on the chain length of the hydrophobic tail. In addition to the results of the present study, therefore, we included the data on C<sub>16</sub>Me<sub>3</sub>ABr that we previously obtained by the same technique.<sup>23</sup>

At the outset, we address the following question: Is there a detectable contribution to the values of  $D_{\text{obs}}$  from free ferrocene, that is, the ferrocene outside the micellar domain? This question is relevant in view of the large difference between  $D_{\text{elect}}$  and  $D_{\text{mic}}$  (the former is ca. 10 times greater than the latter),<sup>27</sup> so a (possible) contribution from the free electroactive species cannot be overlooked: the solubility of ferrocene in water. Three pieces of information show that the above-mentioned contribution can be safely neglected; these are the low solubility of ferrocene in bulk water (see the Experimental Section), its strong binding

to the micelle, the large molar concentration ratio of surfactant to ferrocene employed. The association constants between C<sub>x</sub>Me<sub>3</sub>ABr micelles and ferrocene are large, for example, 1738 and 344 for C<sub>16</sub>Me<sub>3</sub>ABr and C<sub>12</sub>Me<sub>3</sub>ABr, respectively. These values were calculated as indicated elsewhere, by using a (linear) solvation free energy relationship<sup>49</sup> based on the solute parameters of ferrocene.<sup>50</sup> Additionally, the surfactant/ferrocene concentration ratio was maintained high enough ( $\geq 80$ ) to secure complete probe inclusion within the aggregate, at a ratio of one probe molecule per micelle, (Note: As written before, One probe/micelle does not necessarily exclude ferrocene in the bulk solution.)

Figure 2 shows voltammograms recorded for C<sub>14</sub>Me<sub>3</sub>ABr solutions at three different surfactant and ferrocene concentrations. These voltammograms present well-defined sigmoidal profiles, typical of systems controlled by diffusion. A similar behavior was observed for C<sub>10</sub>Me<sub>3</sub>ABr and C<sub>12</sub>Me<sub>3</sub>ABr (voltammograms not shown).

For a surfactant solution, the value of  $D_{\text{obs}}$  depends on the concentrations of the surfactant and additive, if present. Figure 3 shows that  $D_{\text{obs}}$  decreases linearly as a function of increasing surfactant concentration, as a result of intermicelle interactions.<sup>34</sup> The dependence of  $D_{\text{obs}}$  on the NaBr concentration (KBr for C<sub>16</sub>Me<sub>3</sub>ABr) for all surfactants studied is presented in Figure 4. For C<sub>10</sub>Me<sub>3</sub>ABr, C<sub>12</sub>Me<sub>3</sub>ABr, and C<sub>14</sub>Me<sub>3</sub>ABr,  $D_{\text{obs}}$  increases and then decreases as a function of increasing NaBr concentration. A similar, but less pronounced, behavior is observed for C<sub>16</sub>Me<sub>3</sub>ABr, as a function of increasing KBr concentration. We interpret this behavior in terms of two opposing effects: a reduction in electrostatic drag and an increase in micellar size. The electrostatic screening by the added electrolyte attenuates the micellar surface charge, causing a decrease in electrostatic drag; this is responsible for the initial increase in aggregate mobility. Concurrently, the increase of  $N_{\text{agg}}$  as a function of

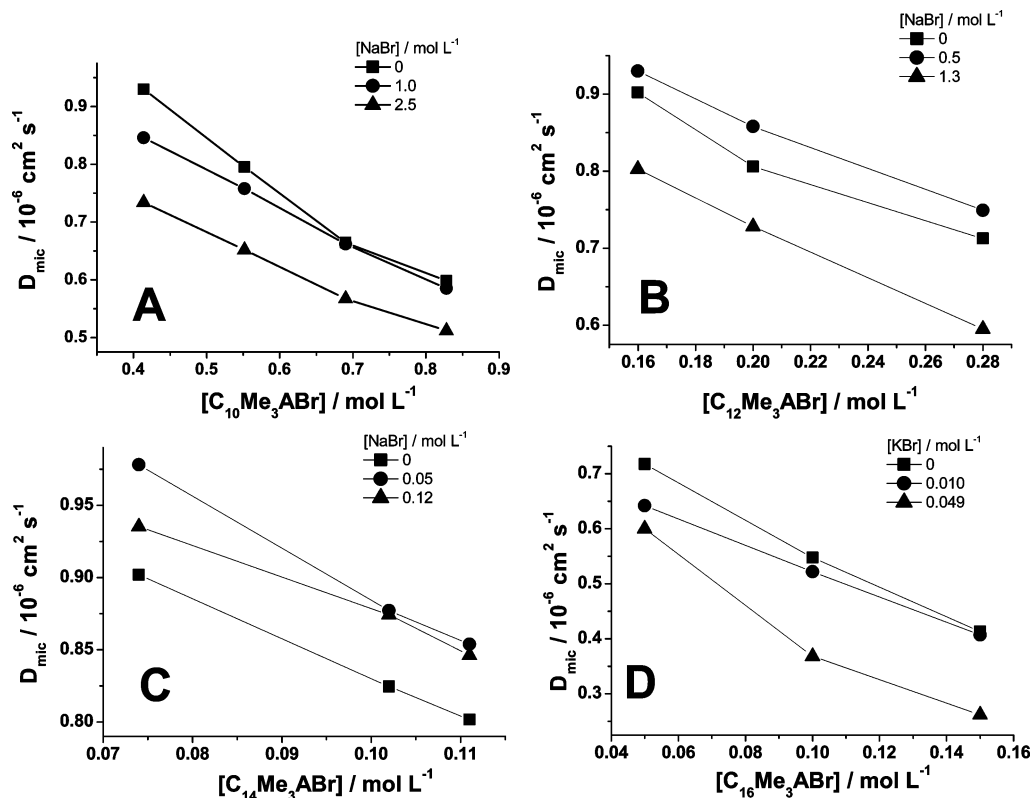


**Figure 5.** Dependence of the diffusion coefficients of (A) C<sub>10</sub>Me<sub>3</sub>ABr, (B) C<sub>12</sub>Me<sub>3</sub>ABr, (C) C<sub>14</sub>Me<sub>3</sub>ABr, and (D) C<sub>16</sub>Me<sub>3</sub>ABr on the surfactant concentration at three different concentrations of bromide.



**TABLE 3: Parameters Obtained in the Absence of Electrolyte for All Surfactants at Their Respective cmc Values**

surfactant	$D^0$ ( $10^{-6}$ cm <sup>2</sup> s <sup>-1</sup> )	$R_H$ (Å)	$N_{agg}$		
			measured	theoretical	from the literature
C <sub>10</sub> Me <sub>3</sub> ABr	1.23 ± 0.05	18 ± 1	42 ± 4	34	40 <sup>48</sup>
C <sub>12</sub> Me <sub>3</sub> ABr	1.16 ± 0.05	18.8 ± 0.9	55 ± 3	51	56, <sup>48</sup> 51, <sup>60</sup> 57 <sup>61</sup>
C <sub>14</sub> Me <sub>3</sub> ABr	1.08 ± 0.05	20.2 ± 0.8	69 ± 3	70	74, <sup>48</sup> 71, <sup>60</sup> 70 <sup>61</sup>
C <sub>16</sub> Me <sub>3</sub> ABr	0.86 ± 0.05	25 ± 1	96 ± 5 <sup>23</sup>	89	95, <sup>48</sup> 91, <sup>60</sup> 101 <sup>61</sup>

increasing electrolyte concentration results in an increase in the micellar size, leading to a decrease in  $D_{obs}$  and, eventually, a sphere-to-rod transition.<sup>51–53</sup> Figure 4 and Table 2 show that the electrolyte concentration required to increase the dimension of the micelles is inversely dependent on the chain length of the surfactant hydrophobic tail. That is, shorter-chain surfactants are less sensitive to the presence of electrolyte.

Values of  $D_{cmc}$  were calculated from the dependence of  $D_{obs}$  on surfactant concentration, and the results are shown in Figure 5, in the absence and presence of additional electrolyte (NaBr or KBr). We used the former data to calculate the micellar hydrodynamic radius using the Stokes–Einstein relation (eq 2). The micellar volume was then calculated according to the equation

$$V_{mic} = \frac{4\pi(R_H^0)^3}{3} \quad (4)$$

The values of  $N_{agg}$  for C<sub>x</sub>Me<sub>3</sub>ABr micelles were calculated by using the equation

$$N_{agg} = V_{mic}/\nu_{mon} \quad (5)$$

where  $\nu_{mon}$  is the volume of a single surfactant monomer, taken as 594.6, 521.2, and 465.1 Å<sup>3</sup> for C<sub>14</sub>-, C<sub>12</sub>-, and C<sub>10</sub>Me<sub>3</sub>ABr, respectively; the latter was calculated by extrapolation of a linear plot of  $\nu_{mon}$  versus the number of carbon atoms of the surfactant hydrophobic chain.<sup>57</sup> MV-based  $N_{agg}$  values are collected in Table 3, along with theoretically calculated aggregation numbers,  $N_{agg,theor}$ , and those obtained using other techniques. The MV-based  $N_{agg}$  values are in excellent agreement with these other

values, as shown by the following slopes and correlation coefficient 0.959, 0.986 ( $N_{agg,theor}$ ) and 0.969, 0.992 ( $N_{agg,literature}$ ).

Values of the intermicellar interaction coefficient ( $k_D$ ) were calculated from the slope of the  $D_{obs}$  versus surfactant concentration plots (Figure 6), as described by linear interaction theory. The repulsive interactions among micelles are gradually attenuated with the addition of electrolytes, resulting in an asymptotic decrease of  $k_D$  as observed for C<sub>10</sub>Me<sub>3</sub>ABr. On the other hand, an unexpected increase in  $k_D$  values was observed for C<sub>12</sub>Me<sub>3</sub>ABr, C<sub>14</sub>Me<sub>3</sub>ABr, and C<sub>16</sub>Me<sub>3</sub>ABr. This is attributed to the sphere-to-rod morphology change; under these experimental conditions, linear interaction theory is no longer applicable.<sup>19</sup>

All results obtained—cmc and  $N_{agg}$  values and sphere-to-rod transitions—indicate a clear dependence on the chain length of the surfactant hydrophobic tail, as well as on the presence of added electrolyte. The increase in  $N_{agg}$  as a function of increasing the length of the R group is due to an increase in the so-called “packing factor”, because such an increase affects the volume of the hydrophobic group more than its length (for the same headgroup). This results in a closer packing of the surfactant monomers, accompanied by a linear decrease in the degree of counterion dissociation,  $\alpha$ , and, hence, the micellar surface charge density ( $\partial\alpha/\text{CH}_2 = -0.018$ ,  $r = 0.991$ ).<sup>58</sup> The addition of electrolyte causes a compression of the electrical double layer surrounding the ionic headgroups, which reduces their mutual repulsion in the micelle. As indicated above, this closer packing of the headgroups eventually leads to rodlike cylindrical micelles.<sup>59</sup> Accordingly, the electrolyte concentration that is required to attenuate the electrostatic headgroup repulsion

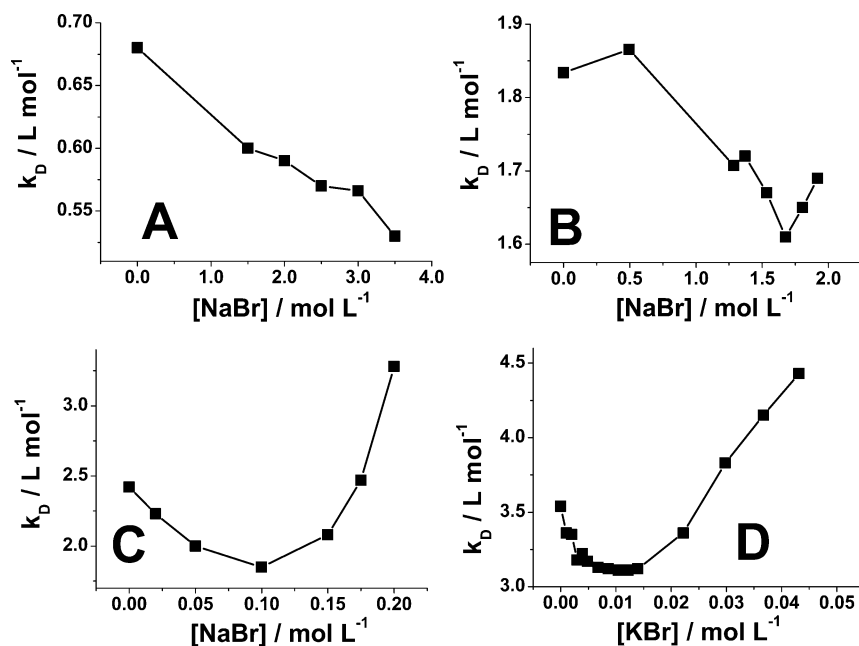


**Figure 6.** Plots of the intermicellar interaction parameter ( $k_D$ ) as a function of bromide concentration for (A) C<sub>10</sub>Me<sub>3</sub>ABr, (B) C<sub>12</sub>Me<sub>3</sub>ABr, (C) C<sub>14</sub>Me<sub>3</sub>ABr, and (D) C<sub>16</sub>Me<sub>3</sub>ABr solutions.

increases fast as a function of increasing the length of R. The linear dependence of the logarithm of the threshold NaBr concentration required to cause micellar morphological changes on the length of R was also studied. From this plot, the NaBr concentration necessary to induce the sphere-to-rod transition for  $C_{10}Me_3ABr$  was calculated, and its value,  $18.3 \text{ mol L}^{-1}$ , is higher than the solubility of NaBr in water.

## Conclusion

MV is a simple and convenient technique for probing fundamental properties of micellar solutions, in particular, their dependence on the chain length of the hydrophobic tail and the presence of additives. Ferrocene is a convenient electroactive probe because of its negligible solubility in water and strong association with micelles. The power of this technique was demonstrated by comparing the micellar properties of  $C_xMe_3ABr$  ( $x = 10\text{--}16$ ) with literature-reported and theoretically calculated values.

**Acknowledgment.** This work was supported by FAPESP (Fundação de Amparo à Pesquisa de São Paulo), CAPES (Coordenação de Aperfeiçoamento de Pessoal de Nível Superior), and CNPq (Conselho Nacional de Desenvolvimento Científico e Tecnológico). We thank Dr. Paulo A. R. Pires for his help with the calculations of  $N_{\text{agg,theor}}$  and the LCCA-USP for making the computing programs available to us.

**Supporting Information Available:** Pictorial representation of micelle-bound ferrocene diffusion to the microelectrode surface. This information is available free of charge via the Internet at <http://pubs.acs.org>.

## References and Notes

- (1) Magid, L. J.; Han, Z.; Warr, G. G.; Cassidy, M. A.; Butler, P. D.; Hamilton, W. A. *J. Phys. Chem. B* **1997**, *101*, 7919.
- (2) Hassan, P. A.; Yakhmi, J. V. *Langmuir* **2000**, *16*, 7187.
- (3) Kabir-ud, D.; Kumar, S.; Kirti, Goyal, P. S. *Langmuir* **1996**, *12*, 1490.
- (4) Kabir-ud, D.; Kumar, S.; Aswal, V. K.; Goyal, P. S. *J. Chem. Soc., Faraday Trans.* **1996**, *92*, 2413.
- (5) Kumar, S.; Bansal, D.; Kabir-ud, D. *Langmuir* **1999**, *15*, 4960.
- (6) El Seoud, O. A. *J. Mol. Liq.* **1997**, *72*, 85.
- (7) Hines, J. D. *Curr. Opin. Colloid Interface Sci.* **2001**, *6*, 350.
- (8) Meyer, E. E.; Rosenberg, K. J.; Israelachvili, J. *Proc. Natl. Acad. Sci. U.S.A.* **2006**, *103*, 15739.
- (9) Charlton, I. D.; Doherty, A. P. *Colloids Surf. A: Physicochem. Eng. Aspects* **2001**, *182*, 305.
- (10) Charlton, I. D.; Doherty, A. P. *J. Phys. Chem. B* **2000**, *104*, 8327.
- (11) Dorshow, R. B.; Bunton, C. A.; Nicoli, D. F. *J. Phys. Chem.* **1983**, *87*, 1409.
- (12) Corti, M.; Degiorgio, V. *J. Phys. Chem.* **1981**, *85*, 711.
- (13) Aswal, V. K.; Goyal, P. S. *Physica B* **1998**, *245*, 73.
- (14) Leaist, D. G.; Hao, L. *J. Phys. Chem.* **1994**, *98*, 4702.
- (15) Stilbs, P. *Prog. Nucl. Magn. Reson. Spectrosc.* **1987**, *19*, 1.
- (16) Mandal, A. B.; Nair, B. U. *J. Phys. Chem.* **1991**, *95*, 9008.
- (17) Mandal, A. B.; Nair, B. U.; Ramaswamy, D. *Langmuir* **1988**, *4*, 736.
- (18) Charlton, I. D.; Doherty, A. P. *Anal. Chem.* **2000**, *72*, 687.
- (19) Charlton, L. D.; Doherty, A. P. *Langmuir* **1999**, *15*, 5251.
- (20) Yang, Z. Y.; Lu, Y.; Zhao, J. S.; Gong, Q. T.; Yin, X. L. *J. Phys. Chem. B* **2004**, *108*, 7523.

- (21) Yang, Z. Y.; Zhao, J. S.; Lu, Y.; Du, X. G. *Anal. Lett.* **2004**, *37*, 2251.
- (22) Yang, Z. Y.; Zhao, J. S.; Lu, Y.; Du, Z. K. *Chem. Phys.* **2004**, *307*, 71.
- (23) Ferreira, T. L.; El Seoud, O. A.; Bertotti, M. *J. Electroanal. Chem.* **2007**, *603*, 275.
- (24) Ferreira, T. L.; El Seoud, O. A.; Bertotti, M. *Electrochim. Acta* **2004**, *50*, 1065.
- (25) Adams, R. N. *Electrochemistry at Solid Electrodes*; Marcel Dekker: New York, 1969.
- (26) Ferreira, T. L.; Paixao, T.; Richter, E. M.; El Seoud, O. A.; Bertotti, M. *J. Phys. Chem. B* **2007**, *111*, 12478.
- (27) Mandal, A. B. *Langmuir* **1993**, *9*, 1932.
- (28) Eddowes, M. J.; Gratzel, M. *J. Electroanal. Chem.* **1984**, *163*, 31.
- (29) Eddowes, M. J.; Gratzel, M. *J. Electroanal. Chem.* **1983**, *152*, 143.
- (30) Zana, R.; Mackay, R. A. *Langmuir* **1986**, *2*, 109.
- (31) Zana, R. *Colloids Surf. A: Physicochem. Eng. Aspects* **1997**, *123*, 27.
- (32) Zana, R. *Surfactants in Solution*; Plenum Press: New York, 1984; Vol. 4.
- (33) Zana, R.; Lang, J. *Solution Behavior of Surfactants*; Plenum Press: New York, 1980; Vol. 2.
- (34) Dickinson, E. *Annu. Rep. Prog. Chem. C* **1983**, *3*.
- (35) Evans, D. F.; Wennerström, A. *The Colloidal Domain*, 2nd ed.; Wiley-VCH: Weinheim, Germany, 1999.
- (36) Reck, R. A.; Harwood, H. J.; Ralston, A. W. *J. Org. Chem.* **1947**, *12*, 517.
- (37) Kolthoff, I. M. *Recl. Trav. Chim. Pays-Bas* **1922**, *41*, 615.
- (38) Pedrotti, J. J.; Angnes, L.; Gutz, I. G. R. *Electroanalysis* **1996**, *8*, 673.
- (39) Pons, S.; Fleischmann, M. *Anal. Chem.* **1987**, *59*, A1391.
- (40) Silva, S. M.; Alves, C. R.; Correia, A. N.; Martins, R. M.; Nobre, A. L. R.; Machado, S. A. S.; Mazo, L. H.; Avaca, L. A. *Quim. Nova* **1998**, *21*, 78.
- (41) Stulik, K.; Amatore, C.; Holub, K.; Marecek, V.; Kutner, W. *Pure Appl. Chem.* **2000**, *72*, 1483.
- (42) Bashford, M. T.; Woolley, E. M. *J. Phys. Chem.* **1985**, *89*, 3173.
- (43) Katsu, T. *Colloids Surf.* **1991**, *60*, 199.
- (44) Delrio, J. M.; Pombo, C.; Prieto, G.; Sarmiento, F.; Mosquera, V.; Jones, M. N. *J. Chem. Thermodyn.* **1994**, *26*, 879.
- (45) Tanford, C. J. *J. Phys. Chem.* **1974**, *78*, 2469.
- (46) Mukerjee, P. *Adv. Colloid Interface Sci.* **1967**, *1*, 241.
- (47) Mukerjee, P.; Mysels, K. J. *Critical Micelle Concentrations of Aqueous Surfactant Systems*; Report NSRDS-NBS 36; U.S. Government Printing Office: Washington, DC, 1971.
- (48) Ray, G. B.; Chakraborty, I.; Ghosh, S.; Moulik, S. P.; Palepu, R. *Langmuir* **2005**, *21*, 10958.
- (49) Quina, F. H.; Alonso, E. O.; Farah, J. P. S. *J. Phys. Chem.* **1995**, *99*, 11708.
- (50) Abraham, M. H.; Benjelloun-Dakhama, N.; Gola, J. M. R.; Acree, W. E.; Cain, W. S.; Cometto-Muniz, J. E. *New J. Chem.* **2000**, *24*, 825.
- (51) Tominaga, T.; Nishinaka, M. *J. Chem. Soc., Faraday Trans.* **1993**, *89*, 3459.
- (52) Aswal, V. K.; Goyal, P. S.; Menon, S. V. G.; Dasannacharya, B. A. *Physica B* **1995**, *213*, 607.
- (53) Aswal, V. K.; Goyal, P. S. *Phys. Rev. E* **2003**, *67*, 8.
- (54) Okuda, H.; Imae, T.; Ikeda, S. *Colloids Surf.* **1987**, *27*, 187.
- (55) Zielinski, R.; Ikeda, S.; Nomura, H.; Kato, S. *J. Colloid Interface Sci.* **1988**, *125*, 497.
- (56) Ozeki, S.; Ikeda, S. *J. Colloid Interface Sci.* **1982**, *87*, 424.
- (57) Hansson, P.; Jonsson, B.; Strom, C.; Soderman, O. *J. Phys. Chem. B* **2000**, *104*, 3496.
- (58) Zana, R.; Yiv, S.; Strazielle, C.; Lianos, P. *J. Colloid Interface Sci.* **1981**, *80*, 208.
- (59) Rosen, M. J. *Surfactants and Interfacial Phenomena*, 2nd ed.; John Wiley and Sons: New York, 1989.
- (60) Rafati, A. A.; Gharibi, H.; Iloukhani, H.; Safdari, L. *Phys. Chem. Liq.* **2003**, *41*, 227.
- (61) Hansson, P.; Almgren, M. *J. Phys. Chem.* **1996**, *100*, 9038.

JP909655Y